

# Fermi-Löwdin orbital self-interaction correction using the strongly constrained and appropriately normed meta-GGA functional

Yoh Yamamoto\*, Carlos M. Diaz\*<sup>§</sup>, Luis Basurto\*, Koblar

A. Jackson<sup>†</sup>, Tunna Baruah\*<sup>§</sup>, and Rajendra R. Zope\*<sup>§a)</sup>

*\*Department of Physics, The University of Texas at El Paso, El Paso, Texas, 79968*

*§Computational Science Program, The University of Texas at El Paso, El Paso, Texas, 79968 and*

*†Physics Department and Science of Advanced Materials Program, Central Michigan University, Mt. Pleasant Michigan, 48859\**

(Dated: October 1, 2019)

## Abstract

Despite the success of density functional approximations (DFAs) in describing the electronic properties of many-electron systems, the most widely used approximations suffer from self-interaction errors (SIE) that limit their predictive power. Here we describe the effects of removing SIE from the strongly constrained and appropriately normed (SCAN) meta-generalized gradient approximation (GGA) using the Fermi-Löwdin Orbital Self-Interaction Correction (FLOSIC) method. FLOSIC is a size-extensive implementation of the Perdew-Zunger self-interaction correction (PZ-SIC) formalism. We find that FLOSIC-SCAN calculations require careful treatment of numerical details and describe an integration grid that yields reliable accuracy with this approach. We investigate the performance of FLOSIC-SCAN for predicting a wide array of properties and find that it provides better results than FLOSIC-LDA and FLOSIC-PBE in nearly all cases. It also gives better predictions than SCAN for orbital energies and dissociation energies where self-interaction effects are known to be important, but total energies and atomization energies are made worse. For these properties, we also investigate the use of the self-consistent FLOSIC-SCAN density in the SCAN functional and find that this DFA@FLOSIC-DFA approach yields improved results compared to pure, self-consistent SCAN calculations. Thus FLOSIC-SCAN provides improved results over the parent SCAN functional in cases where SIEs are dominant, and even when they are not, if the SCAN@FLOSIC-SCAN method is used.

---

\* <sup>a)</sup> rzope@utep.edu

## I. INTRODUCTION

Density functional theory (DFT) has been widely used to study the electronic structure of various types of materials from atoms and molecules to nanostructures to periodic materials. The popularity of DFT stems from its low computational expense combined with relatively good accuracy. The self-interaction error (SIE) that arises from the density functional approximations (DFAs) of the exchange-correlation functional is well-documented [1]. This error arises since the self-Coulomb energy is not completely canceled by the self-exchange energy when the exact, but unknown, exchange-correlation functional is approximated. This leads to a number of problems. For example, the one-electron potential in DFA does not have the correct asymptotic behavior due to the presence of the SIE, leaving the highest occupied orbitals in stable anions unbound as a result.

The Perdew-Zunger self-interaction correction formalism (PZ-SIC) is a one-electron self-interaction-free approximation where an orbital by orbital correction is applied to the DFA total energy [1]. A number of implementations of SIC to DFT exist [2–19], including a recent implementation by Jónsson *et al.* using complex orbitals that has shown promising results [20]. The PZ-SIC formalism corrects SIE, but it also leads to an orbital-dependent theory since the orbital-dependent total energy is not invariant under a unitary transformation of the occupied orbitals. The set of orbitals that yields the minimum self-interaction corrected total energy therefore must be found. Pederson *et al.* showed that these minimum-energy local orbitals satisfy additional pairwise conditions known as the localization equations (LE) [21, 22]. Varying the  $N^2$  elements of a unitary transformation to find local orbitals that satisfy the LE is a process that scales poorly with increasing numbers of orbitals, making the solution of the LE computationally challenging. Another problem with traditional PZ-SIC is that it is not formally size-extensive. The canonical Kohn-Sham (KS) orbitals tend to delocalize with increasing system size. In the limit of very large sizes and very delocalized orbitals, the correction terms in PZ-SIC tend to zero[23]. This leads to a breakdown of size extensivity when the lowest-energy correction for a single atom is positive.

An alternative approach to solving the LE in PZ-SIC was introduced by Pederson, Perdew, and Ruzsinszky through the use of Fermi-Löwdin orbitals (FLO) [24] to evaluate the PZ-SIC total energy. (The resulting method is known as FLOSIC.) The FLOs are orthonormal local orbitals that are a linear combination of Fermi orbitals (FO). The FOs

depend on the density matrix and spin density at certain points in space called Fermi orbital descriptors (FODs). The FOs are obtained from the KS orbitals as

$$\phi_{i\sigma}^{FO}(r) = \frac{\sum_j^{N_\sigma} \psi_{j\sigma}^*(\mathbf{a}_{i\sigma}) \psi_{j\sigma}(\vec{r})}{\sqrt{\rho_\sigma(\mathbf{a}_{i\sigma})}} \quad (1)$$

where  $\psi_{j\sigma}$ ,  $\rho_\sigma$ ,  $\mathbf{a}_{i\sigma}$ ,  $N_\sigma$  denote KS orbital, total electron density, FOD, and number of occupied orbitals of spin  $\sigma$ , respectively. The FO transformation is unitarily invariant, *i.e.* the same set of FO's is produced by any orthonormal set of orbitals spanning the occupied space. The total energy in FLOSIC therefore depends on the FOD positions and the LE do not need to be applied. In addition, because the FLOs are localized, the FLOSIC method restores size extensivity [24].

The FO are determined by the positions of the FODs; therefore, only  $3N$  variables are needed to determine the optimal set of local orbitals, compared to  $N^2$  coefficients of a unitary transformation needed in traditional PZ-SIC. Thus, in principle, FLOSIC provides a computationally simpler way to incorporate the self-interaction correction. In practical FLOSIC calculations, optimal FOD positions are found using gradients of the energy with respect to FOD positions, in a procedure analogous to molecular geometry optimizations [25, 26]. A number of studies have been conducted using the FLOSIC method [24, 27–34].

To date, FLOSIC has been applied mostly to the LDA level of theory where nearly all properties of atoms and molecules are significantly improved [25, 27, 35]. On the other hand, SIC-based improvements are known to be less uniform with semilocal generalized gradient approximations (GGA) and meta-GGAs [12, 36, 37]. Recently, Perdew and coworkers have provided insight into this problem [37], showing that the lobed one electron densities needed for applying SIC are problematic for semilocal functionals such as the Perdew, Burke, and Ernzerhof (PBE) [38, 39] GGA and the strongly constrained and appropriately normed (SCAN) [40, 41] meta-GGA. While the use of complex orbitals can lessen the problem, it does not eliminate it [37]. In related work, Santra and Perdew showed applying SIC to a semilocal functional causes appropriate norms that are built in to the functional to be violated [42].

Because these recent developments may lead to new approaches to implementing SIC and because SCAN is the most successful nonempirical semilocal functional for predicting the properties of atoms, molecules, and solids, it is important to thoroughly benchmark the

performance of SCAN when used with the existing FLOSIC methodology. We note that although some initial applications of FLOSIC-SCAN were included in the recent publications [37, 42], this article presents the details of the FLOSIC-SCAN implementation for the first time, including a description of refinements to the numerical integration grid that are necessary to insure accurate results. It also gives a full account of how FLOSIC-SCAN performs for a number of properties such as atomic energies,  $\Delta$ -SCF ionization potentials and electron affinities, ionization potential estimates from the HOMO energies of atoms and molecules, dissociation energies using benchmark sets that are known to be sensitive to SIEs, and atomization energies. In all cases, we compare the performance of FLOSIC-SCAN to that of FLOSIC-LDA and FLOSIC-PBE and the uncorrected SCAN functional. We also examine the effectiveness of using FODs optimized at the FLOSIC-LDA level in FLOSIC-SCAN calculations.

Finally, we also investigate the quality of the self-consistent FLOSIC-DFA electron density by using it in place of the corresponding self-consistent DFA density in the parent DFA functional. Since the FLOSIC method restores the correct asymptotic behavior to the DFA potential for a localized system, it is expected to improve the quality of the density in the asymptotic region. Hence, the more physically correct electron density from FLOSIC, when combined with an accurate functional such as SCAN, may lead to improved estimates of total energies by removing density driven errors [43, 44]. Our results show that using the FLOSIC density in the parent functional often leads to electronic properties near equilibrium that are improved over those of the parent functional.

This article is organized as follows. In Sec. II, we present our computational method and also discuss the implementation of SCAN in the FLOSIC code. Calculated data for the atoms and their ionization potentials and electron affinities using the FLOSIC method are discussed in Sec. III A. FLOSIC total and atomization energies of selected molecules are presented and discussed in Sec. III B. FLOSIC dissociation energies are presented in Sec. III C. Finally in Sec. III D, we discuss the eigenvalues of the highest occupied molecular orbitals using FLOSIC.

## II. COMPUTATIONAL METHOD

All of the results presented in this manuscript are calculated with the FLOSIC code, which is based on the UTEP version of the NRLMOL code [45], a Gaussian orbital-based electronic structure code [46–48]. Among the features included in this version is an interface to the exchange-correlation library called LIBXC. The latter provides access to a large number exchange-correlation functionals [49, 50]. The FLOSIC code inherits the optimized Gaussian basis sets of NRLMOL [51] and an accurate numerical integration grid scheme [46]. In all of our calculations, the default NRLMOL basis sets are used. A recent study which studied ionization potentials and enthalpies of formation using FLOSIC approach, the default NRLMOL basis set was found to provide results comparable to the cc-pVQZ basis set [52]. The SIC calculations require finer mesh as orbital densities are involved in calculation of orbital dependent potentials. A default NRLMOL mesh for FLOSIC calculation, on average, has 25000 grid points per atom. This results in integration of charge density that is accurate to the order of  $10^{-8}e$ . The exchange-correlation (XC) functionals used in this study are the LSDA implementation of Perdew and Wang (LDA) [53], Perdew, Burke & Ernzerhof (PBE) [38, 39], and SCAN [41].

FLOSIC calculations require an initial set of trial FOD positions. Whenever they are available, previously reported FOD positions are used as starting points. In other cases, FODs are generated from scratch and further optimized using a conjugate gradient algorithm. We use the convergence criteria of  $10^{-6}$  Ha on the FLOSIC total energy for these optimizations. We find that FLOSIC-LDA optimized FOD positions are typically a good starting point for FLOSIC-PBE and FLOSIC-SCAN calculations. For example, the FOD positions for neutral atoms shifted an average of only 0.073 Bohr after optimization with FLOSIC-SCAN, while keeping similar overall arrangements.

Meta-GGA functionals, including SCAN, are sensitive to the numerical details of a calculation, and this sensitivity extends to FLOSIC-SCAN calculations. The standard variational integration mesh method [46] employed in the FLOSIC code provides good accuracy for the LSDA and PBE functionals, but not for SCAN calculations. Semilocal meta-GGA functionals use a dimensionless variable defined as

$$\alpha = \frac{\tau - \tau^W}{\tau^{\text{unif}}} > 0 \tag{2}$$

where  $\tau$  is the kinetic energy density,  $\tau^W = |\vec{\nabla}\rho|^2/8\rho$  is the Weizsäcker kinetic energy density, and  $\tau^{\text{unif}} = (3/10)(3\pi^2)^{2/3}\rho^{5/3}$  is the kinetic energy density at the uniform-density limit. The numerical challenges of using SCAN are related to changes in  $\alpha$ . Recently, Bartók and Yates showed that the numerical instabilities arising from switching function in SCAN can be eliminated by modifying the switching function [54]; however, such modification results in violation of some exact constraints. The exchange enhancement factor of SCAN has a mathematical form given as

$$F_x(s, \alpha) = \{h_x^1(s, \alpha) + f_x(\alpha)[h_x^0 - h_x^1(s, \alpha)]\}g_x(s), \quad (3)$$

$$f_x(\alpha) = \exp\left[-\frac{c_{1x}\alpha}{1-\alpha}\right]\theta(1-\alpha) - d_x \exp\left[\frac{c_{2x}}{1-\alpha}\right]\theta(\alpha-1), \quad (4)$$

$$s = \frac{|\vec{\nabla}\rho|}{2(3\pi^2)^{1/3}\rho^{4/3}} \quad (5)$$

where  $h_x^1(s, \alpha)$  is a function of  $s$  and  $\alpha$ ,  $g_x(s)$  is a function of  $s$ ,  $h_x^0 = 1.174$ ,  $s$  is dimensionless density gradient,  $c_{1x}$ ,  $c_{2x}$ ,  $d_x$  are interpolation parameters, and  $\theta(x)$  is a step function of  $x$  [41]. Figure 1 shows  $f_x(\alpha)$  (Eq. (4)) and its derivative,  $\frac{df_x(\alpha)}{d\alpha}$ , as functions of  $\alpha$ . A large oscillation of  $\frac{df_x(\alpha)}{d\alpha}$  is seen near  $\alpha = 1$ . A high density of grid points is needed in the areas where the  $\frac{df_x(\alpha)}{d\alpha}$  term changes rapidly in space, and similarly for the  $\frac{df_c(\alpha)}{d\alpha}$  function used in the correlation term. The enhanced mesh used in the FLOSIC code was designed to provide this. To obtain numerically converged results, following procedure was adopted. We begin by adding radial points with uniform increments until the integrals are converged. This is a brute force approach of mesh generation. This is done to eliminate any assumption about the problematic ( $\alpha \approx 1$ ) region. We then decrease the number of radial grid points in the region farther from the nuclei by maintaining the same grid density in the problematic ( $\alpha \approx 1$ ) region. It is ensured that the integrals accuracy remains same ( $10^{-8}$  Ha for exchange-correlation energy) while reducing the grid density. This approach has worked well but still results in a numerical mesh that is approximately three to six times larger than the default variational mesh. The SCAN mesh used in this work is roughly 140000 grid points per atom. This results in integration of charge density which is accurate in the order of  $10^{-10}e$ . Further improvement of the numerical grid to reduce the need of such dense grid is being explored and will be reported in future.

### A. Meta-GGA implementation

The meta-GGA exchange-correlation energy has the form given as

$$E_{XC}[\rho_{\uparrow}, \rho_{\downarrow}] = \int e_{XC}(\rho_{\uparrow}, \rho_{\downarrow}, \vec{\nabla}\rho_{\uparrow}, \vec{\nabla}\rho_{\downarrow}, \tau_{\uparrow}, \tau_{\downarrow}) d\vec{r} \quad (6)$$

where  $e_{XC}$  is the exchange-correlation energy density function,  $\rho_{\uparrow}$  and  $\rho_{\downarrow}$  are electron spin densities, and  $\tau_{\uparrow}$  and  $\tau_{\downarrow}$  are kinetic energy density. The kinetic energy density is calculated from the KS orbitals  $\psi_i$  as

$$\tau(\vec{r}) = \frac{1}{2} \sum_i \vec{\nabla}\psi_i(\vec{r}) \cdot \vec{\nabla}\psi_i(\vec{r}). \quad (7)$$

To obtain the exchange-correlation potential, functional derivatives of  $E_{XC}$  are required. In the case of Eq. (6), the functional derivative of exchange-correlation energy with respect to density is

$$\begin{aligned} \frac{\delta E_{XC}[\rho]}{\delta \rho(\vec{r})} &= \frac{\partial e_{XC}(\rho(\vec{r}), \vec{\nabla}\rho(\vec{r}), \tau(\vec{r}))}{\partial \rho(\vec{r})} - \vec{\nabla} \frac{\partial e_{XC}(\rho(\vec{r}), \vec{\nabla}\rho(\vec{r}), \tau(\vec{r}))}{\partial \vec{\nabla}\rho(\vec{r})} \\ &+ \int \frac{\partial e_{XC}(\rho(\vec{r}'), \vec{\nabla}\rho(\vec{r}'), \tau(\vec{r}'))}{\partial \tau(\vec{r}')} \frac{\delta \tau[\rho](\vec{r}')}{\delta \rho(\vec{r})} d\vec{r}' \end{aligned} \quad (8)$$

where the third term is obtained with the functional derivative chain rules. Typically, an exchange-correlation functional is implemented in quantum chemistry software in such a way that  $\frac{\partial e_{XC}(\rho, \vec{\nabla}\rho, \tau)}{\partial \rho}$ ,  $\frac{\partial e_{XC}(\rho, \vec{\nabla}\rho, \tau)}{\partial \vec{\nabla}\rho}$ , and  $\frac{\partial e_{XC}(\rho, \vec{\nabla}\rho, \tau)}{\partial \tau}$  are returned from subroutines. The  $\frac{\delta \tau[\rho](\vec{r}')}{\delta \rho}$  in Eq. (8) can be calculated as  $\frac{\delta \tau}{\delta \psi} \frac{\delta \psi}{\delta \rho}$ ; however, computing  $\frac{\delta \psi[\rho](\vec{r}')}{\delta \rho}$  is difficult. It was suggested by Zahariev *et al.* [55] and Yang *et al.* [56] that the Hamiltonian matrix elements of the pure meta-GGA exchange-correlation potential can be written as follows, using integrations-by-parts:

$$\begin{aligned} &\int \psi_i(\vec{r}) \frac{\delta E_{XC}[\tau[\rho]]}{\delta \rho(\vec{r})} \psi_j(\vec{r}) d\vec{r} \\ &\approx \frac{1}{2} \int \frac{\delta E_{XC}[\tau]}{\delta \tau(\vec{r})} \vec{\nabla}\psi_i(\vec{r}) \cdot \vec{\nabla}\psi_j(\vec{r}) d\vec{r}. \end{aligned} \quad (9)$$

This approach of computing the Hamiltonian matrix elements is used for the meta-GGA implementation in the FLOSIC code.

## B. FLOSIC

FLOSIC uses the PZ-SIC total energy expression that removes the self-interaction of the occupied orbitals on an orbital by orbital basis:

$$E^{SIC}[\rho_{\uparrow}, \rho_{\downarrow}] = E[\rho_{\uparrow}, \rho_{\downarrow}] - \sum_{\sigma} \sum_i^{N_{\sigma}} \left( U[\rho_{i\sigma}] + E_{XC}[\rho_{i\sigma}, 0] \right) \quad (10)$$

where  $\sigma$  is the spin index,  $i$  is the orbital index, and  $N_{i\sigma}$  is the number of orbitals for spin  $\sigma$ .  $\rho_{\uparrow}$  and  $\rho_{\downarrow}$  denote spin up and spin down electron densities.  $\rho_{i\sigma} = |\phi_{i\sigma}|^2$ , where the  $\phi_{i\sigma}$  are the Fermi-Löwdin orbitals (FLO). The FO are constructed from a transformation on the KS orbitals using Eq. (1). These are normalized, but not mutually orthogonal. Löwdin orthogonalization yields the FLOs.

The DFA-SIC single particle equations are

$$(H_{\sigma}^{DFA} + V_{i\sigma}^{SIC})\phi_{i\sigma} = \sum_j^{N_{\sigma}} \lambda_{ji\sigma} \phi_{j\sigma}. \quad (11)$$

These are satisfied self-consistently for a given choice of the FODs, following the approach of Ref. [35]. We use an SCF convergence tolerance of  $10^{-6}$  Ha.

## III. RESULTS AND DISCUSSION

### A. Atoms: total energies, ionization energies, and electron affinities

The focus of this work is to give a comprehensive assessment of the results of FLOSIC-SCAN calculations. To do that we compare these to corresponding results for FLOSIC-LDA, FLOSIC-PBE, and for the corresponding uncorrected DFA's.

The FLOSIC energies for atoms from H–Ar ( $Z = 1 - 18$ ) can be compared against accurate non-relativistic total energies reported by Chakravorty *et al.* [57]. The deviation of the calculated total energies are given on a per electron basis as  $(E - E_{\text{Ref}})/N_e$ , where  $E$  is the FLOSIC energy,  $E_{\text{Ref}}$  is the reference energy, and  $N_e$  is the number of electrons in the given system. The results are shown in Fig. 2–4, and the numerical errors of FLOSIC energies with respect to  $E_{\text{Ref}}$  are presented in Table I. As noted in earlier works [24, 26, 27],



we find that the total energies with LSDA improve within the FLOSIC method (shown in Fig. 2) with a decrease in mean absolute error (MAE) from 0.73 Ha (LSDA) to 0.38 Ha (FLOSIC-LSDA). On the other hand, both PBE and SCAN total energies show a larger deviation when corrected for self-interaction using FLOSIC as shown in Figures 3 and 4. The MAEs for total energy with PBE and FLOSIC-PBE are 0.083 and 0.159 Ha respectively; for SCAN and FLOSIC-SCAN the MAE's are 0.019 and 0.15 Ha. Thus, FLOSIC-PBE and FLOSIC-SCAN perform better than LSDA and FLOSIC-LSDA, but not as well as PBE and SCAN.

DFT calculation using accurate electron densities can eliminate density driven errors and give better energies [43, 58]. Since SIC restores the correct asymptotic behavior of the potential and one-electron self-interaction freedom [42], it can provide a more physically reasonable density than a DFA calculation. It is therefore of interest to calculate the total energies using the self-consistent FLOSIC density in the standard GGA (PBE) and meta-GGA (SCAN) functionals. We denote these results as DFA@FLOSIC-DFA. For example, the SCAN@FLOSIC-SCAN is the result obtained by using the self-consistent FLOSIC-SCAN electron density to evaluate the SCAN total energy. The DFA@FLOSIC-DFA with LDA, PBE, and SCAN produces atomic total energies that are very close to the self-consistent total energies of the respective DFA as shown in Figs. 2–4. For completeness, we also tested the FLOSIC-LDA and FLOSIC-PBE densities in SCAN. The SCAN@FLOSIC-SCAN, SCAN@FLOSIC-PBE and SCAN@FLOSIC-LDA energies are very close, indicating that the respective FLOSIC densities are similar. Note that these DFA@FLOSIC-DFA results are obtained at no additional computational cost beyond that of the FLOSIC calculations.

We also calculated the ionization potentials (IPs) for H–Kr atoms with FLOSIC applied to the LDA, PBE, and SCAN functionals. The FOD optimization of cations is performed independently, and the resulting cation total energy  $E_{\text{cat}}$  is then used to calculate the IP as

$$E_{\text{IP}} = E_{\text{cat}} - E_{\text{neut}}. \quad (12)$$

The results from FLOSIC-LDA, FLOSIC-PBE, and FLOSIC-SCAN calculations are summarized in Table II, and the energy differences from corresponding experimental energies [59] are shown in Fig. 5. FLOSIC-LDA tends to overestimate the IPs with a few exceptions.

On the other hand, FLOSIC-PBE and FLOSIC-SCAN energies underestimate the experimental values. The mean absolute percentage errors (MAPE) in ionization energies are 7.68, 5.13, and 5.18 % for LDA, PBE, and SCAN, respectively. The MAPE values in IP are 5.01, 5.04, and 3.30 % for FLOSIC-LDA, FLOSIC-PBE, and FLOSIC-SCAN respectively. For all three functionals, the values of IP are reduced overall with SIC compared to without. The IPs of PBE and SCAN are over-corrected with SIC. This is seen in the sign of mean errors (ME); with SIC, the ME in IP changes from 0.342 to  $-0.230$  eV for PBE and from 0.277 to  $-0.278$  eV for SCAN. In terms of mean absolute errors (MAE), FLOSIC improves the MAE for LSDA, from 0.619 to 0.402 eV, but increases it for PBE, from 0.397 to 0.468 eV. The MAE is improved from 0.398 to 0.299 eV for SCAN and FLOSIC-SCAN. The results for LSDA and PBE are consistent with those of Vydrov and Scuseria [13]. By comparing the SIC energy corrections for the neutral atoms and their cations, we observe that the overcorrection of IPs with semilocal functionals occurs because the neutrals have a larger positive correction than the cations, in most cases. We point out that the optimization of the FOD at the level of the meta-GGA is important. We compared our FLOSIC-SCAN results with those calculated using descriptors optimized with FLOSIC-LDA. We find that the IPs with FLOSIC-SCAN show a sizable improvement after performing FOD optimization. The MAE using FLOSIC-LDA optimized FODs is 0.448 eV; this decreases to 0.299 eV upon FLOSIC-SCAN optimization. This reduction comes about in part by improving the Co IP. Using FLOSIC-LDA FODs, the error for Co is  $-5.082$  eV; using FLOSIC-SCAN FODs, the error drops to  $-0.137$  eV. This points to the importance of optimizing the FODs with a consistent functional.

Similarly to what we have done for the total energy of atoms, we performed DFA@FLOSIC-DFA calculations for the IP. PBE@FLOSIC-PBE gives MAPE of 4.91 %, which is a smaller error than both PBE and FLOSIC-PBE. For SCAN@FLOSIC-SCAN (MAPE = 5.28%), we do not see a performance improvement compared to SCAN (5.18%) or FLOSIC-SCAN (3.30%).

Finally, the electron affinities (EA) of the atoms were computed by taking the difference  $EA = E_{\text{neut}} - E_{\text{anion}}$ . For the anion calculations, we added additional single Gaussian orbitals (s, p, and d-type) to the default NRLMOL basis set to account for the more diffuse nature of the anion wave functions. These extra orbitals share the same Gaussian exponents that are obtained using the relation  $\beta(N + 1) = \beta(N)^2 / \beta(N - 1)$  where  $\beta(N)$  is the N-th

Gaussian exponent in the basis. We computed EAs for H, Li, B, C, O, F, Na, Al, Si, P, S, Cl, K, Ti, Cu, Ga, Ge, As, Se, and Br, for which experimental EA values are available in Ref. [60]. In all the DFA anion calculations, the orbital eigenvalue of the highest occupied orbital becomes positive due to SIE [1], implying that the fully charged anions are not truly bound in DFA. Despite this, we adopt the common practice of computing EA values by taking total energy difference of an atom and its anion via  $\Delta$ -SCF. These are listed in Table III and are comparable to those reported by Vydrov and Scuseria [14]. The application of SIC results in negative HOMO orbital energies, due to the improved description of the exchange potential in the asymptotic region. FLOSIC-PBE and FLOSIC-SCAN generally underestimate the EAs as seen from ME and MAE as well as in Fig. 6. Overall, the performance of FLOSIC-LSDA is the best among the three FLOSIC-DFAs.

DFA@FLOSIC-DFA calculations were also performed for EA similarly to the IP calculations. For all three functionals, the errors with respect to experimental values are noticeably reduced compared to the pure DFA calculations (cf. Table III). This suggests that density-driven errors may be particularly important in describing the EA.

## B. Atomization energies

FLOSIC-LDA, -PBE, and -SCAN are also used to calculate the total and atomization energies (AE) of a set of 37 molecules. This supplements the FLOSIC-SCAN results that appeared recently [37]. Most of the molecules are taken from the G2/97 test set [61]; in addition, we include the six molecules from the AE6 test set [62], as well as HBr, LiBr, NaBr, FBr, Br<sub>2</sub>, and cyclopentadienyl. Most of the geometries for these molecules were optimized using B3LYP with the 6-31G(2df,p) basis [60]. The geometries for O<sub>2</sub>, CO, CO<sub>2</sub>, C<sub>2</sub>H<sub>2</sub>, Li<sub>2</sub>, CH<sub>4</sub>, NH<sub>3</sub>, and H<sub>2</sub>O were optimized using the PBE functional and the default NRLMOL basis set. FOD positions were initially optimized using FLOSIC-LDA and further optimized for FLOSIC-SCAN.

The atomization energy of a molecule is defined as

$$E_a = \sum_i^{N_{\text{atom}}} E_i - E_{\text{mol}} > 0 \tag{13}$$

where  $E_i$  is the energy of individual atoms,  $N_{\text{atom}}$  is the number of atoms in the given

molecule, and  $E_{\text{mol}}$  is the total energy of a molecule. Table IV summarizes the errors in calculated AEs for DFA only, FLOSIC-DFA, and DFA@FLOSIC-DFA calculations. The experimental energies are taken from Ref. [60]. The MAEs are 99.0, 65.7, 196.0, 84.3, and 73.7 kJ/mol for PBE, SCAN, FLOSIC-LDA, FLOSIC-PBE, and FLOSIC-SCAN respectively. At the DFA level, SCAN performs much better than PBE resulting in the smallest MAE of 65.7 kJ/mol and MAPE of 5.22 % among all five cases. On the other hand, FLOSIC-PBE and FLOSIC-SCAN results are generally worse than those of their parent functionals. We find that FLOSIC-LDA performs the worst of the above five cases with overestimated AE for many systems and especially for  $\text{Br}_2$  for which the MAPE is 13.42 %. FLOSIC-PBE and FLOSIC-SCAN atomization energies have similar MAEs and MAPEs. It is interesting to note that for FLOSIC-SCAN, the MAE is 94.5 kJ/mol using LDA-optimized FODs and it improves to 73.7 kJ/mol after FOD optimization in FLOSIC-SCAN, indicating again that it is important to optimize FODs at a consistent level of theory.

Application of SIC generally results in an underestimation of the AEs compared to uncorrected DFA calculations (see Fig. 7). This is similar to results seen previously for semilocal functionals [14]. In the FLOSIC calculations with semilocal functionals, we observe that SIC treatment raises the total energies of the molecules more than it raises the combined total energies of separated atoms with a few exceptions. This observation was also noted by Shahi *et al.* for real localized SIC orbitals [37]. Consequently, the SIC treatment lowers atomization energies according to Eq. (13).

We find that DFA@FLOSIC-DFA improves atomization energies with respect to *both* the parent DFA and FLOSIC-DFA calculations. The MAPE in AE for PBE is 8.64% while that for FLOSIC-PBE is 9.67%. The MAPE for PBE@FLOSIC-PBE, on the other hand, is considerably smaller 7.72%. Similar improvement is also observed for SCAN. The MAPE of SCAN@FLOSIC-SCAN (5.05%) is smaller than both the FLOSIC-SCAN (10.24 %) and SCAN (5.22 %).

### C. Dissociation energies

We use SIE11 and SIE4 $\times$ 4 test sets [63, 64], sets of benchmark reactions that are known to be sensitive to self-interaction errors, to investigate the performance of FLOSIC-SCAN on the dissociation energy calculations. The SIE11 test set consists of 11 systems that are

directly affected from SIE. The SIE4×4 set consists of 4 positively charged dimers ( $\text{H}_2^+$ ,  $\text{He}_2^+$ ,  $(\text{NH}_3)_2^+$ , and  $(\text{H}_2\text{O})_2^+$ ) separated at four different distances  $R$  from the equilibrium distances  $R_e$  ( $R/R_e=1.0, 1.25, 1.5, \text{ and } 1.75$ ); this set is designed to capture the effects of pure one-electron SIE. Previously, Sharkas *et al.* studied both SIE11 and SIE4×4 with FLOSIC-LDA and FLOSIC-PBE and found that removal of self-interaction improves the performance in both case [31]. The dissociation energy is given as the difference of the complex total energy  $E(X)$  and the fragments  $E(X^+)$  and  $E(X_2^+)$  as

$$E_D = E(X) + E(X^+) - E(X_2^+). \quad (14)$$

The results are compared against the reference values in Ref. [63] and are shown in Table V. For LDA and PBE, we find MAE decreases from DFA to FLOSIC. The DFA calculations overestimate the total energies of both complexes and fragments, and it leads to large errors in the dissociation energies. FLOSIC is able to correct the total energies and improves errors in dissociation. This is expected since a removal of SIE should improve the results. SCAN has relatively small self-interaction compared to other functionals, and DFA-SCAN shows smaller MAE in SIE11 (10.4 kcal/mol) than that for FLOSIC-LDA (11.7 kcal/mol). In those data sets, the SIC treatment improves the performance of SCAN. We find that FLOSIC-SCAN (MAE = 5.7 kcal/mol for SIE11 and 2.2 kcal/mol for SIE4×4) performs very well among the three functionals under both DFA and FLOSIC.

The SIE11 set is divided into five positively charged cationic and six neutral systems. DFA@FLOSIC-DFA calculations improve the errors for the neutral systems. This implies that those neutral systems are susceptible to density driven errors. For the SIE11 cationic systems, on the other hand, the MAEs of DFA@FLOSIC-DFA fall between FLOSIC and DFA indicating that full SIC treatment is needed. We observed the similar results for SIE4×4 where full SIC is required as this dataset contains stretched bonds.

#### D. Eigenvalues of the highest occupied orbitals

In exact DFT, the negative of the highest occupied eigenvalue equals the first ionization energy of the system [65, 66]. This property has been widely used to adjust the magnitude of the exchange potential or exact exchange potentials in practical DFT calculations [67, 68]. In

Fig. 8 we compare the SCAN and FLOSIC-SCAN HOMO orbital eigenvalues  $\varepsilon_{HO}$  of atoms  $Z = 1-36$  against experimental electron removal energies. We also include the corresponding results for LDA, PBE, FLOSIC-LDA, and FLOSIC-PBE for comparison. Table VI shows that the MAEs of DFA orbital eigenvalues are 4.06, 4.15, and 3.88 eV for LDA, PBE, and SCAN respectively, and MAE of FLOSIC-DFA eigenvalues are 0.67, 0.59, and 0.61 eV in the same order. Although the size of the errors of the HOMO eigenvalues is similar to the errors in IP calculated using total energy differences, the corrections to the HOMO eigenvalues are much larger. The DFA HOMO eigenvalues significantly underestimate the electron removal energies for all three functionals. FLOSIC corrects this and reduces the MAE by a factor of 6 to 7.

Similar improvement in the eigenvalues of the HOMO is also seen for the set of molecules studied here (Fig. 9). As with the atoms, the HOMOs for the molecules are too high, underestimating electron removal energies. In all cases, the HOMO eigenvalues are significantly lowered resulting in overestimated ionization potentials with FLOSIC.

Eliminating self-interaction error improves the description of the potential seen by the electrons in the asymptotic region. This accounts for the significant improvement in the eigenvalue of the highest occupied orbitals as can be seen from Tables VI and VII. As HOMO eigenvalue is related to the asymptotic decay of the electron density [65, 69], it is reasonable to expect that the FLOSIC electron density is more accurate in the valence region than the corresponding uncorrected DFA density.

#### IV. CONCLUSION

We implemented meta-GGA functionals in the FLOSIC code and compared the performance of FLOSIC-SCAN to that of FLOSIC-LDA and FLOSIC-PBE calculations for a variety of properties. Total energies of atoms from H-Kr are obtained. We find that SCAN performs well in the total energy calculations, however, correcting for self-interaction errors using FLOSIC worsens the total energies. As also has been noted in a few earlier PZ-SIC works, the application of the FLOSIC method deteriorates the total energies and atomization energies where self-interaction errors are small. Only in the case of LDA, the removal of self-interaction errors improves the results over the parent DFA functional. For ionization potentials, FLOSIC improves ionization potentials for LDA but worsens them for

PBE and SCAN. A pragmatic solution to obtain meaningful estimates of the atomization and total energies is to compute these quantities using the self-consistent self-interaction corrected electron density and Kohn-Sham orbitals in the parent functional. This perturbative procedure does not require any additional computational effort beyond the FLOSIC calculation. Our results show that the total energies, atomization energies, electron affinities and ionization energies (using  $\Delta$ -SCF) obtained using such a procedure are of comparable quality as of their parent functionals while keeping the benefits from SIC such as physically accurate electron densities and improved occupied orbital eigenvalues. For the SCAN functional, we saw some improvement over DFA-SCAN in total and atomization energies as judged from MAEs of these quantities. The procedure adopted here is similar to that used in removing delocalization errors (density driven errors) in the literature [43] and is expected to be more accurate for ionization potentials and electron affinities for larger systems. The present work shows that FLOSIC calculations can provide accurate estimates of the near equilibrium properties (e.g. total and atomic energies) where SIE are small by employing DFA@FLOSIC-DFA approach while providing accurate description of properties like dissociation energies (using full FLOSIC-DFA) where SIC errors are large. Alternative approaches to rectify the overcorrection of the PZ-SIC/FLOSIC methods are being pursued in our laboratory.

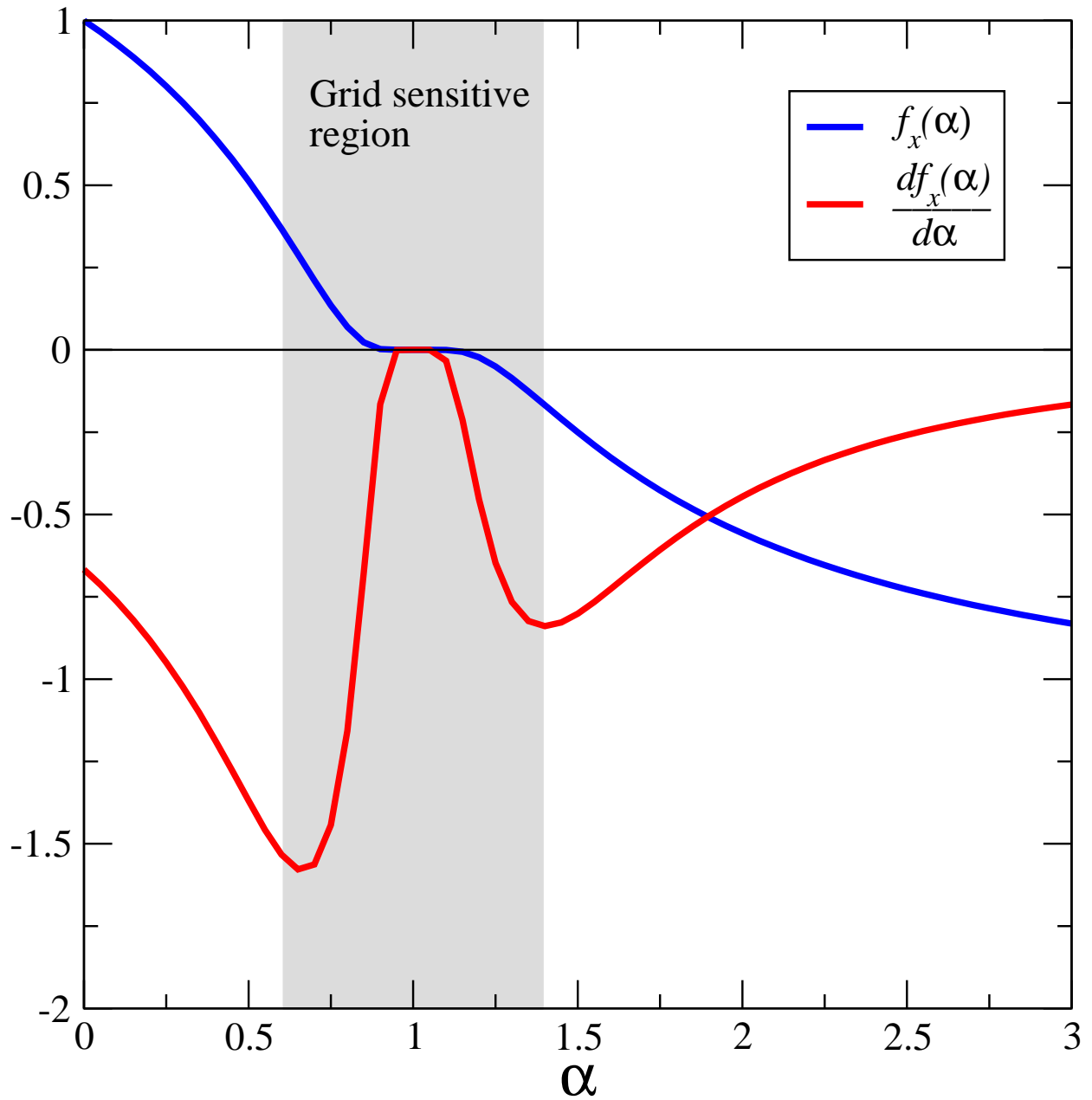


FIG. 1: A plot of  $f_x(\alpha)$  (Eq. 4) and  $df_x(\alpha)/d\alpha$  used in the SCAN exchange enhancement factor. A large oscillation of  $df_x(\alpha)/d\alpha$  is seen near  $\alpha = 1$ .



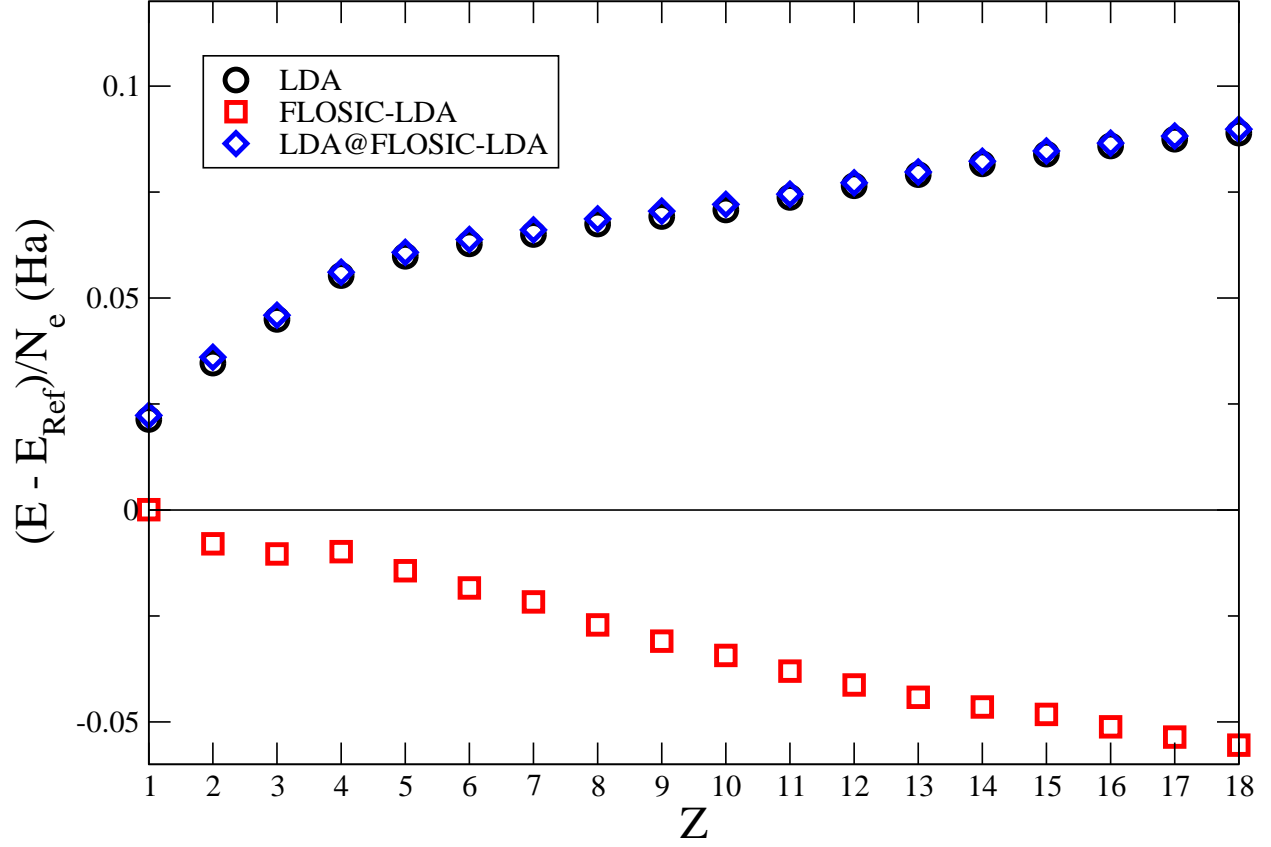


FIG. 2: Atomic total energies (in Ha) for LDA (black circles), FLOSIC-LDA (red squares), and LDA@FLOSIC-LDA (blue diamonds), compared against the reference values of Ref. [57].  $(E - E_{\text{Ref}})/N_e$  is shown, where  $N_e$  is the number of electrons.

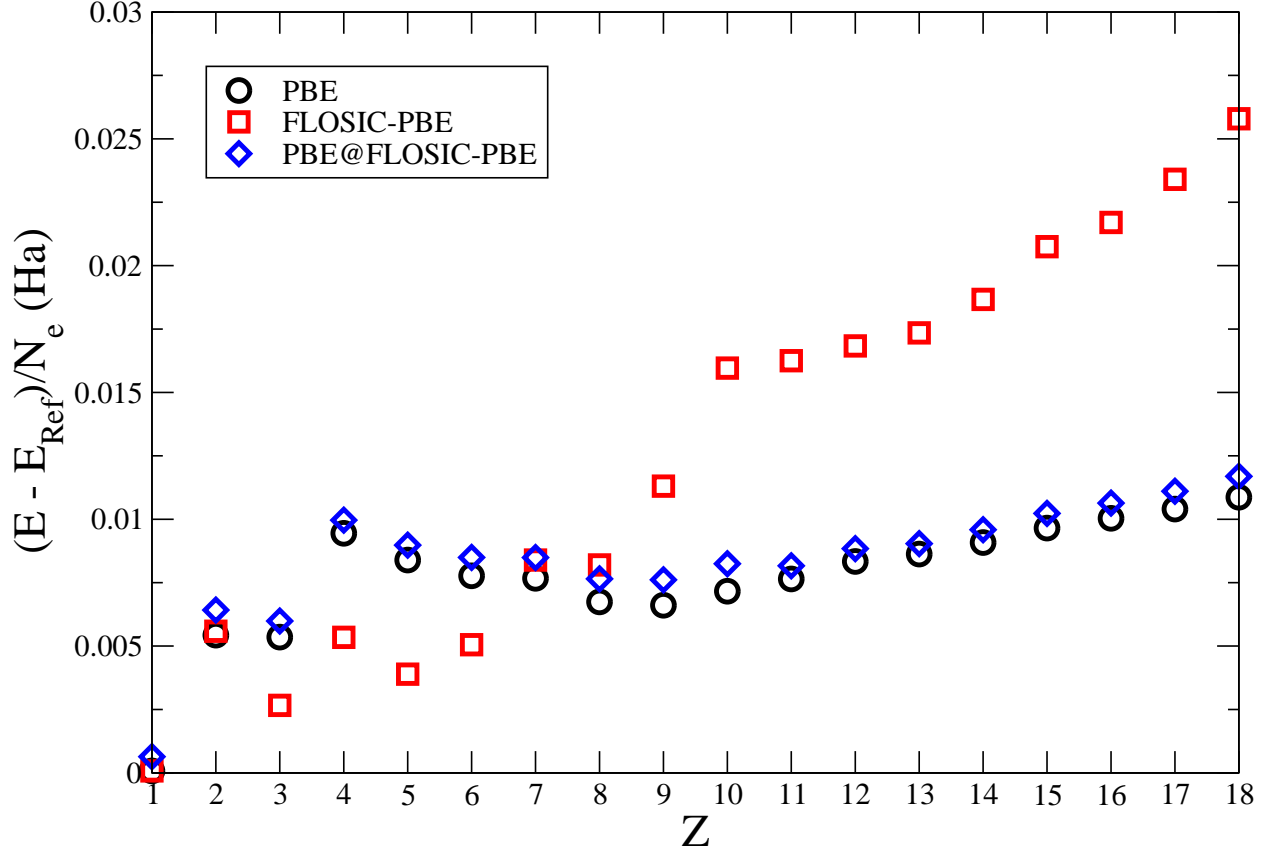


FIG. 3: Atomic total energies (in Ha) for PBE (black circles), FLOSIC-PBE (red squares), and PBE@FLOSIC-PBE (blue diamonds), compared against the reference values of Ref. [57].  $(E - E_{\text{Ref}})/N_e$  is shown, where  $N_e$  is the number of electrons.

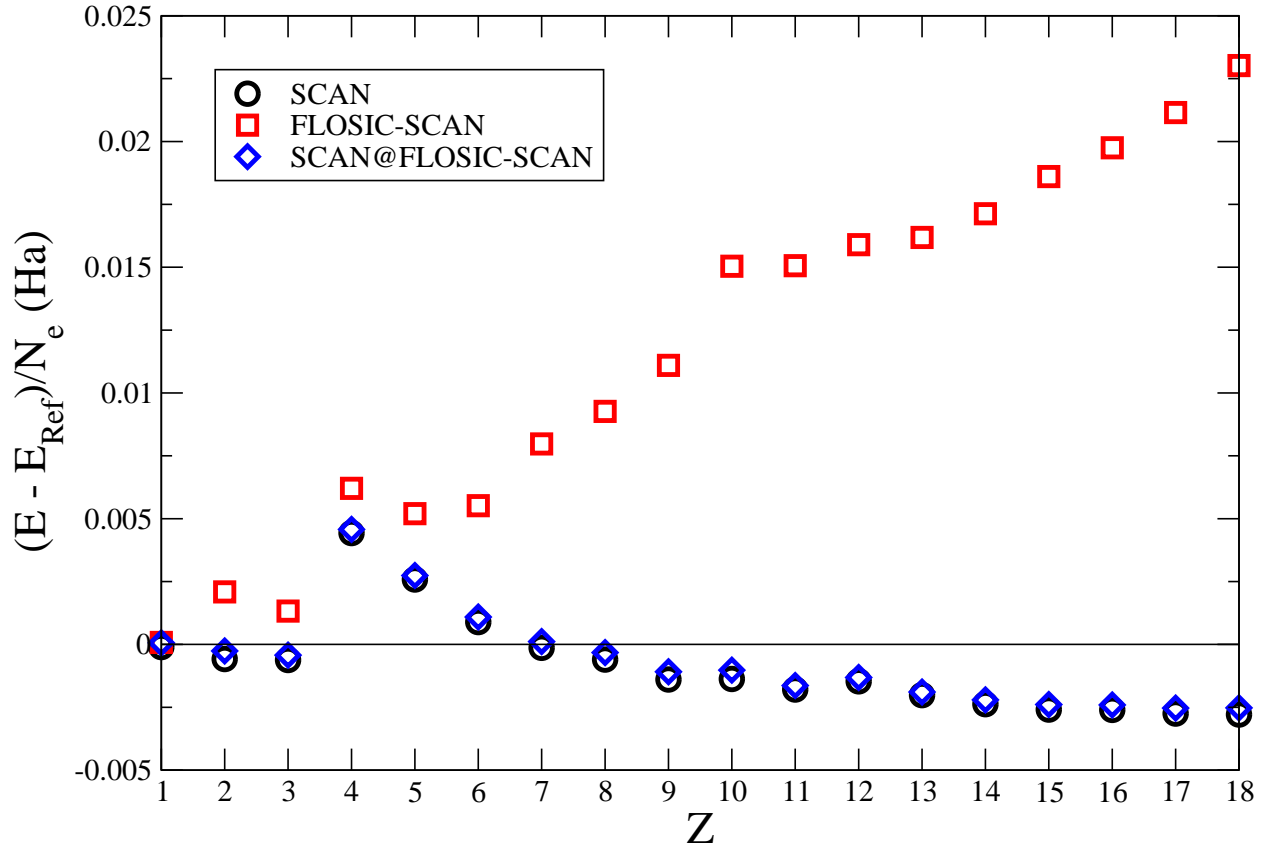


FIG. 4: Atomic total energies (in Ha) for SCAN (black circles), FLOSIC-SCAN (red squares), and SCAN@FLOSIC-SCAN (blue diamonds) compared against the reference values of Ref. [57].  $(E - E_{\text{Ref}})/N_e$  is shown, where  $N_e$  is the number of electrons.

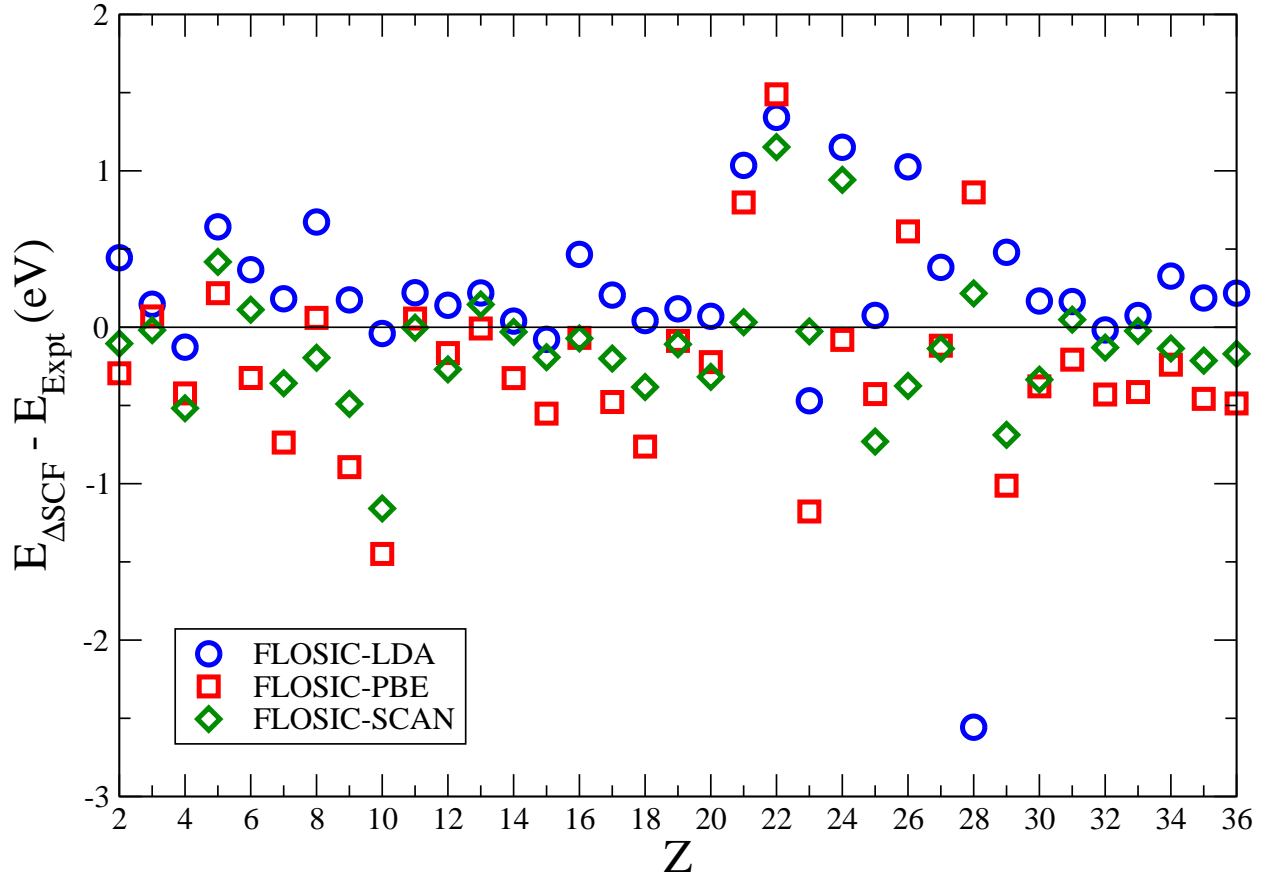


FIG. 5: Ionization energies (in eV) of atoms computed using FLOSIC-LDA (blue circles), FLOSIC-PBE (red squares), and FLOSIC-SCAN (green diamonds). The energies are obtained by  $\Delta$ -SCF and compared against the experimental values of Ref. [59].

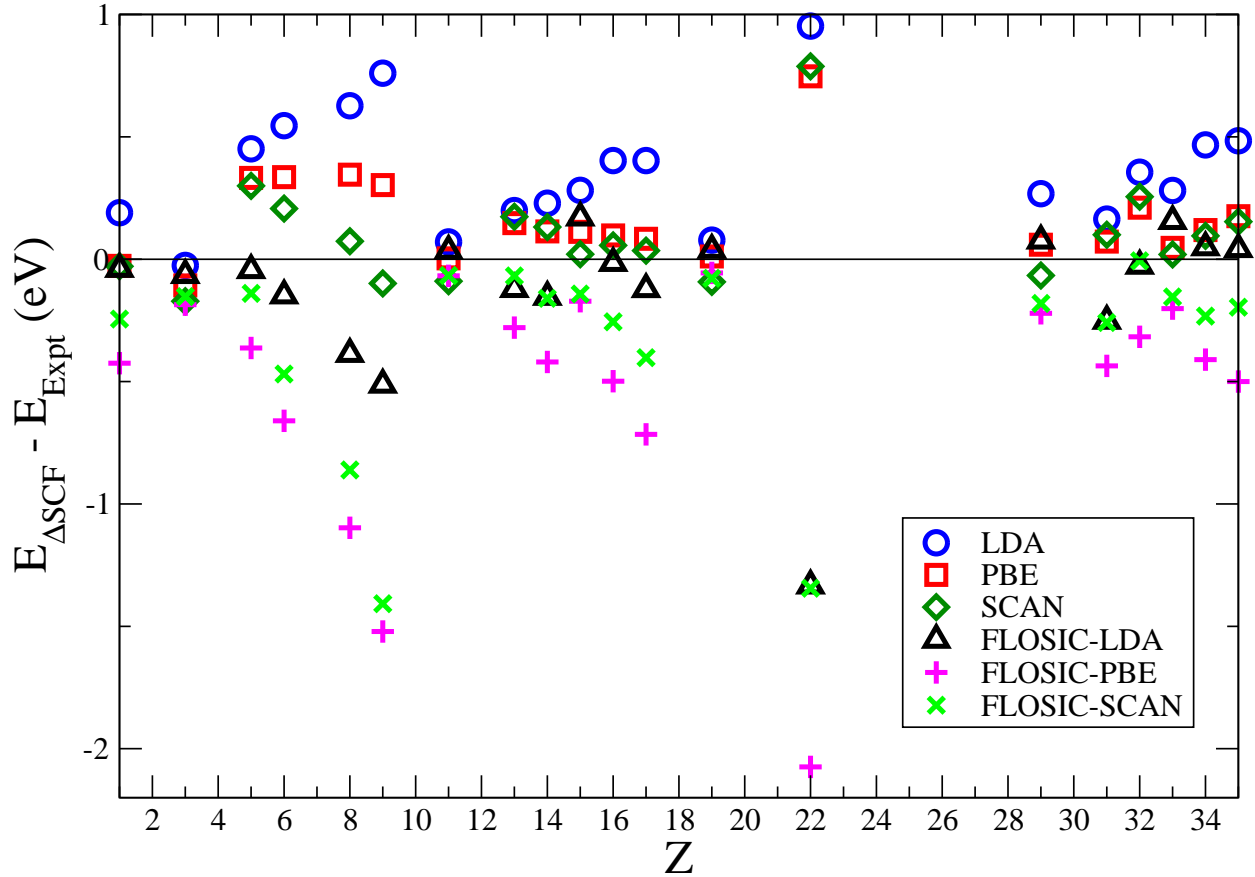


FIG. 6: Electron affinities (in eV) of 20 atoms computed using LDA (blue circles), PBE (red squares), SCAN (green diamonds), FLOSIC-LDA (black triangles), FLOSIC-PBE (magenta crosses), and FLOSIC-SCAN (green xs). The energies are obtained by  $\Delta$ -SCF and compared against the experimental values of Ref. [60].

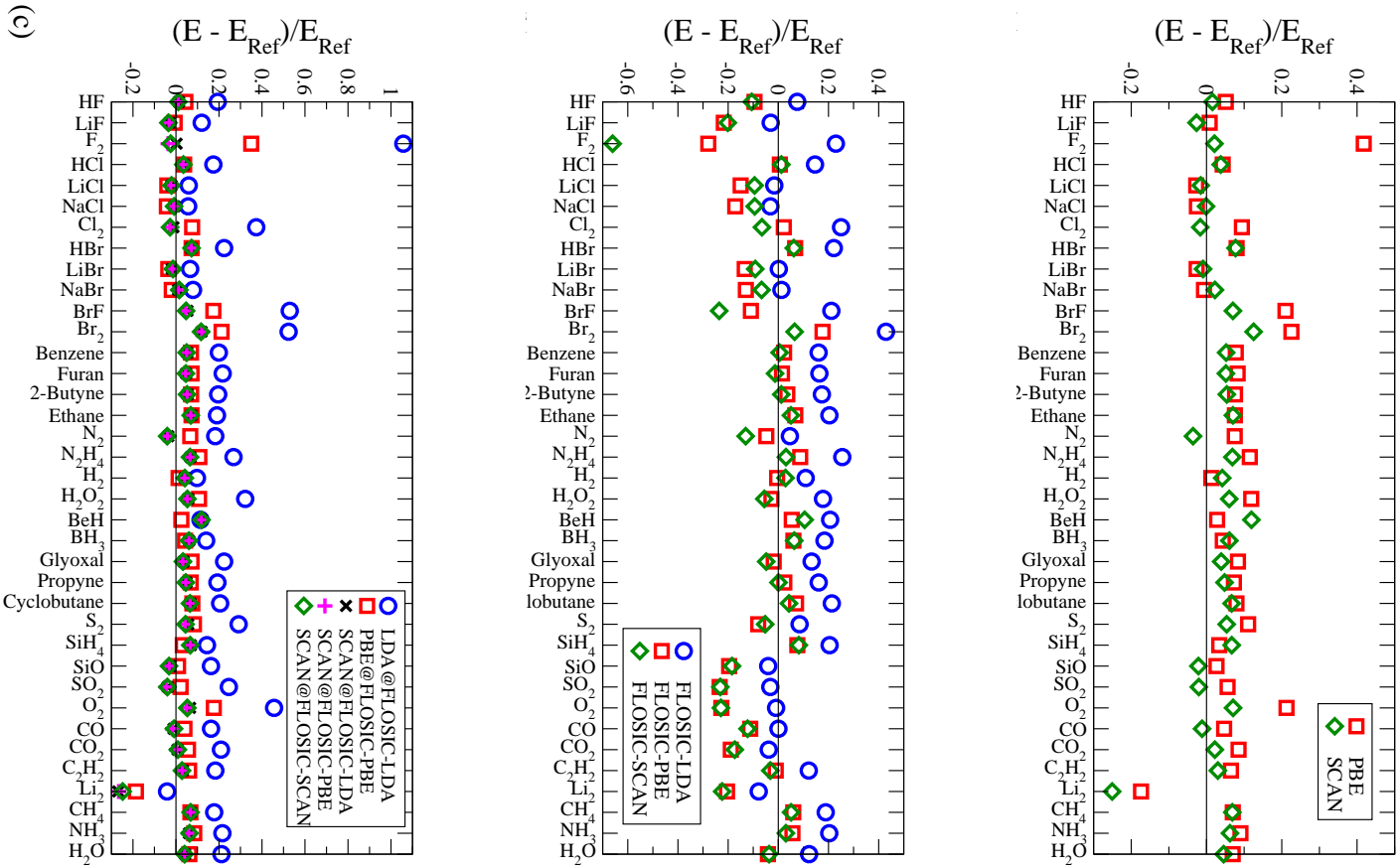


FIG. 7: Atomization energies of molecules compared against reference experimental values found in Ref. [60].  $(E - E_{\text{Ref}})/E_{\text{Ref}}$  is shown: (a) DFA, (b) FLOSIC, and (c) DFA@FLOSIC-DFA.

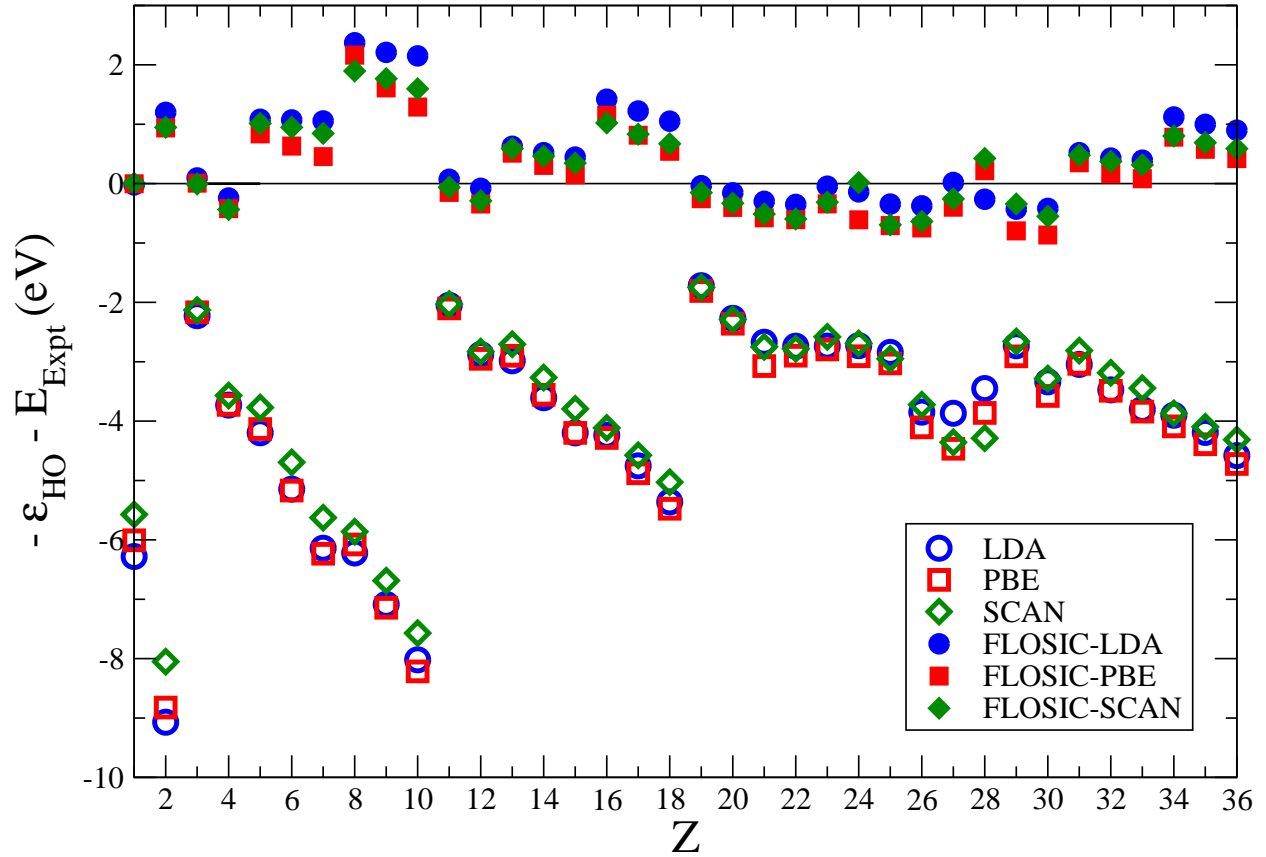


FIG. 8: Deviation of  $-\epsilon_{HO}$  from the corresponding experimental ionization potential[59] (in eV) for atoms with  $Z = 1 - 36$ . LDA (blue circles), PBE (red squares), SCAN (green diamonds), FLOSIC-LDA (filled blue circles), FLOSIC-PBE (filled red squares), and FLOSIC-SCAN (filled green diamonds) values are shown.

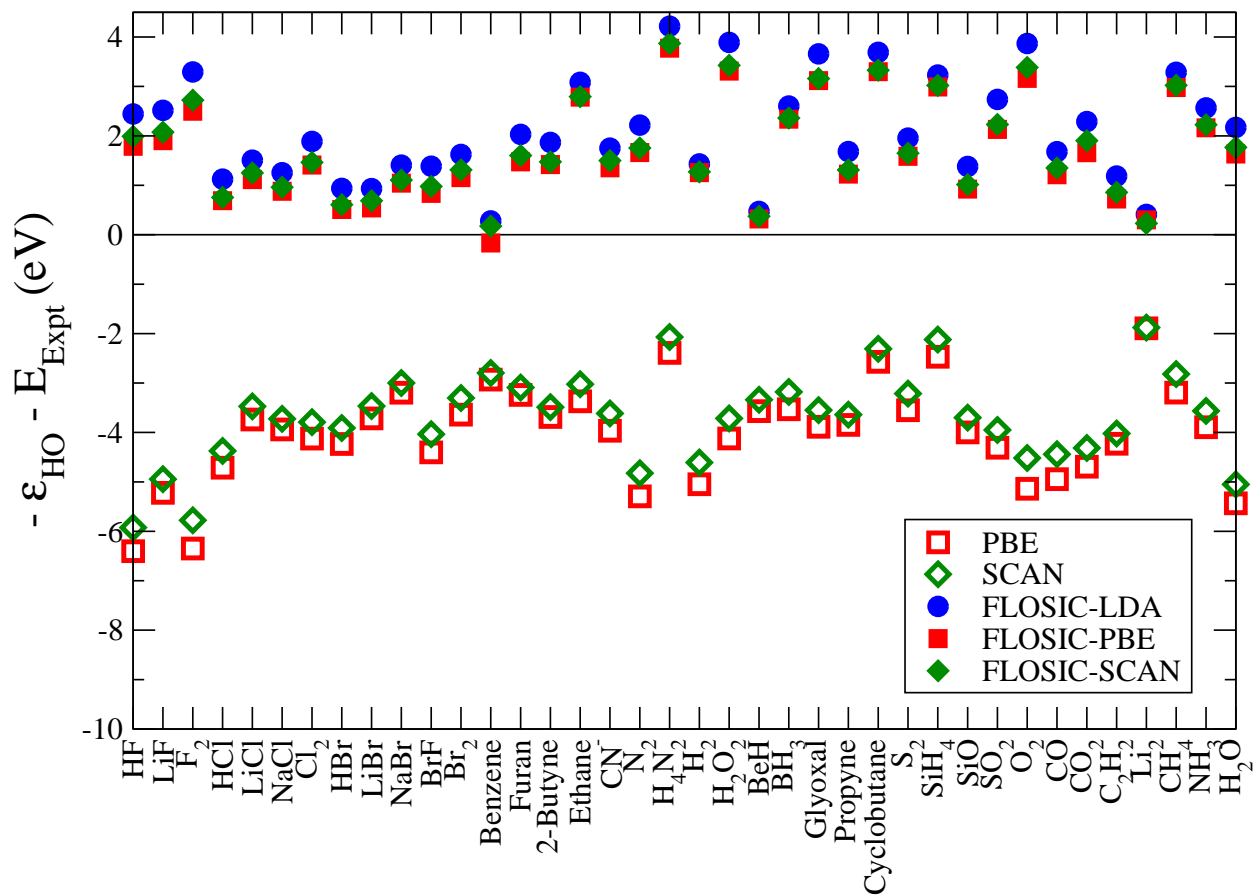


FIG. 9: Deviation of  $-\epsilon_{HO}$  from the corresponding experimental ionization potential (in eV) for a test set of molecules. The experimental values are from Ref. [70] and Ref. [71].

PBE (red squares), SCAN (green diamonds), FLOSIC-LDA (filled blue circles), FLOSIC-PBE (filled red squares), and FLOSIC-SCAN (filled green diamonds) values are shown.



## TABLES

TABLE I: Mean absolute error (MAE in Ha) of the total energies of atoms with  $Z = 1 - 18$  calculated with various methods when compared against reference values given in Ref. [57].

Method	MAE (Ha)
LDA	0.726125
FLOSIC-LDA	0.380502
LDA@FLOSIC-LDA	0.734249
PBE	0.082958
FLOSIC-PBE	0.159131
PBE@FLOSIC-PBE	0.089404
SCAN	0.019197
FLOSIC-SCAN	0.147113
SCAN@FLOSIC-SCAN	0.017547

TABLE II: Deviation of calculated ( $\Delta$ -SCF) ionization potentials from experimental values for atoms  $Z = 2 - 36$  for several methods. Mean errors (ME, in eV), mean absolute errors (MAE, in eV), and mean absolute percentage errors (MAPE) are shown.

Method	ME (eV)	MAE (eV)	MAPE (%)
LDA	0.586	0.619	7.68
FLOSIC-LDA	0.214	0.402	5.01
LDA@FLOSIC-LDA	0.482	0.521	6.45
PBE	0.342	0.397	5.13
FLOSIC-PBE	-0.230	0.468	5.04
PBE@FLOSIC-PBE	0.272	0.372	4.91
SCAN	0.277	0.398	5.18
FLOSIC-SCAN (LDA FOD)	-0.278	0.448	5.17
FLOSIC-SCAN (Optimized FOD)	-0.123	0.299	3.30
SCAN@FLOSIC-SCAN (LDA FOD)	0.244	0.402	5.28
SCAN@FLOSIC-SCAN (Optimized FOD)	0.241	0.402	5.28

TABLE III: Electron affinities of 20 atoms calculated with various methods and compared to experimental values [60]. Mean error (ME) and mean absolute error (MAE) are shown, both in eV.

Method	ME	MAE
LDA	0.359	0.362
FLOSIC-LDA	-0.133	0.189
LDA@FLOSIC-LDA	0.227	0.231
PBE	0.159	0.172
FLOSIC-PBE	-0.531	0.531
PBE@FLOSIC-PBE	0.038	0.080
SCAN	0.093	0.148
FLOSIC-SCAN	-0.341	0.341
SCAN@FLOSIC-SCAN	0.031	0.126

TABLE IV: Atomization energies for the test set of molecules featured in Fig. 7. Mean absolute errors (MAE, in kJ/mol), mean percentage errors (MPE), mean absolute percentage errors (MAPE), and root mean square errors (RMS, in kJ/mol) are shown.

Method	MAE (kJ/mol)	MPE (%)	MAPE (%)	RMS (kJ/mol)
FLOSIC-LDA	195.95	11.93	13.42	321.16
LDA@FLOSIC-LDA	267.41	22.78	23.00	381.49
PBE	98.99	7.24	8.64	146.48
FLOSIC-PBE	84.30	-4.81	9.67	114.21
PBE@FLOSIC-PBE	88.85	5.93	7.72	133.27
SCAN	65.69	3.01	5.22	102.42
FLOSIC-SCAN (LDA FOD)	94.50	-4.84	10.45	131.78
FLOSIC-SCAN (Optimized FOD)	73.72	-6.78	10.24	97.83
SCAN@FLOSIC-SCAN (LDA FOD)	63.38	2.31	5.10	98.82
SCAN@FLOSIC-SCAN (Optimized FOD)	62.84	2.35	5.05	97.87

TABLE V: SIE11 and SIE4×4 dissociation energies calculated by various methods and compared to reference values from Ref. [63]. Mean absolute errors (MAE, in kcal/mol) of SIE11 (5 cationic, 6 neutral, and 11 combined systems) and SIE4×4 are shown.

Method	SIE11, 5 cationic	SIE11, 6 neutral	SIE11	SIE4×4
LDA	22.9	13.4	17.8	27.5
FLOSIC-LDA	14.8	9.0	11.7	3.0
LDA@FLOSIC-LDA	20.1	8.9	14.1	21.2
PBE	12.7	10.9	12.1	23.3
FLOSIC-PBE	8.9	6.4	7.5	3.4
PBE@FLOSIC-PBE	9.6	4.5	7.2	15.1
SCAN	10.4	9.9	10.4	17.9
FLOSIC-SCAN	5.1	6.2	5.7	2.2
SCAN@FLOSIC-SCAN	8.8	4.9	6.9	12.4

TABLE VI: Deviation of  $-\varepsilon_{HO}$  from the corresponding experimental ionization potential for atoms with  $Z = 1 - 36$ . Mean errors (ME) and mean absolute errors (MAE) are given in eV.

Method	ME	MAE
LDA	-4.059	4.059
PBE	-4.150	4.150
SCAN	-3.880	3.880
FLOSIC-LDA	0.494	0.672
FLOSIC-PBE	0.189	0.590
FLOSIC-SCAN (LDA FODs)	0.314	0.622
FLOSIC-SCAN (FOD optimized)	0.318	0.606

TABLE VII: Deviation of  $-\varepsilon_{HO}$  from the corresponding experimental ionization potential for the set of molecules featured in Fig. 9. Mean errors (ME) and mean absolute errors (MAE) are given in eV.

Method	ME	MAE
PBE	-4.023	4.023
SCAN	-3.699	3.699
FLOSIC-LDA	2.104	2.104
FLOSIC-PBE	1.658	1.667
FLOSIC-SCAN (LDA FODs)	1.790	1.790
FLOSIC-SCAN (Optimized FOD)	1.762	1.762

## SUPPLEMENTARY MATERIAL

See supplementary material for detailed results of the total energies, IP, EA, Atomization energies, and  $-\varepsilon_{HO}$  for the systems studied in this manuscript and detailed results for SIE11, SIE4 $\times$ 4, and BH6 molecular test sets.

## ACKNOWLEDGMENTS

The authors gratefully acknowledge discussions with Profs. Mark R. Pederson, John Perdew, Jianwei Sun, and Dr. Jorge Vargas. The initial phase of the work (implementation of meta-GGAs) was supported by the Office of Basic Energy Sciences, U.S. Department of Energy de-sc0002168 and de-sc0006818 while the applications using FLOSIC are supported by de-sc0018331 as a part of the Computational Chemical Sciences program. This research used resources of the National Energy Research Scientific Computing Center (NERSC), a U.S. Department of Energy Office of Science User Facility operated under Contract No. DE-AC02-05CH11231.

- 
- [1] J. P. Perdew and A. Zunger, *Phys. Rev. B* **23**, 5048 (1981).
- [2] J. Garza, J. A. Nichols, and D. A. Dixon, *J. Chem. Phys.* **112**, 7880 (2000), <https://doi.org/10.1063/1.481421>.
- [3] J. Garza, R. Vargas, J. A. Nichols, and D. A. Dixon, *J. Chem. Phys.* **114**, 639 (2001), <https://aip.scitation.org/doi/pdf/10.1063/1.1327269>.
- [4] S. Patchkovskii, J. Autschbach, and T. Ziegler, *J. Chem. Phys.* **115**, 26 (2001), <https://doi.org/10.1063/1.1370527>.
- [5] S. Patchkovskii and T. Ziegler, *J. Chem. Phys.* **116**, 7806 (2002), <https://doi.org/10.1063/1.1468640>.
- [6] S. Patchkovskii and T. Ziegler, *J. Phys. Chem. A* **106**, 1088 (2002), <https://doi.org/10.1021/jp014184v>.
- [7] S. Goedecker and C. J. Umrigar, *Phys. Rev. A* **55**, 1765 (1997).
- [8] V. Polo, E. Kraka, and D. Cremer, *Mol. Phys.* **100**, 1771 (2002), <https://doi.org/10.1080/00268970110111788>.
- [9] V. Polo, J. Gräfenstein, E. Kraka, and D. Cremer, *Theor. Chem. Acc.* **109**, 22 (2003).
- [10] J. Gräfenstein, E. Kraka, and D. Cremer, *J. Chem. Phys.* **120**, 524 (2004), <https://doi.org/10.1063/1.1630017>.
- [11] J. Gräfenstein, E. Kraka, and D. Cremer, *Phys. Chem. Chem. Phys.* **6**, 1096 (2004).
- [12] O. A. Vydrov and G. E. Scuseria, *J. Chem. Phys.* **121**, 8187 (2004), <https://aip.scitation.org/doi/pdf/10.1063/1.1794633>.
- [13] O. A. Vydrov and G. E. Scuseria, *J. Chem. Phys.* **122**, 184107 (2005), <https://doi.org/10.1063/1.1897378>.
- [14] O. A. Vydrov, G. E. Scuseria, J. P. Perdew, A. Ruzsinszky, and G. I. Csonka, *J. Chem. Phys.* **124**, 094108 (2006), <https://doi.org/10.1063/1.2176608>.
- [15] O. A. Vydrov and G. E. Scuseria, *J. Chem. Phys.* **124**, 191101 (2006), <https://doi.org/10.1063/1.2204599>.
- [16] T. Tsuneda, M. Kamiya, and K. Hirao, *J. Comput. Chem.* **24**, 1592 (2003), <https://onlinelibrary.wiley.com/doi/pdf/10.1002/jcc.10279>.
- [17] J. B. Krieger, Y. Li, and G. J. Iafrate, *Phys. Rev. A* **45**, 101 (1992).

- [18] J. B. Krieger, Y. Li, and G. J. Iafrate, *Phys. Rev. A* **46**, 5453 (1992).
- [19] Y. Li, J. B. Krieger, and G. J. Iafrate, *Phys. Rev. A* **47**, 165 (1993).
- [20] S. Lehtola, M. Head-Gordon, and H. Jónsson, *J. Chem. Theory Comput.* **12**, 3195 (2016), pMID: 27232582, <https://doi.org/10.1021/acs.jctc.6b00347>.
- [21] M. R. Pederson, R. A. Heaton, and C. C. Lin, *J. Chem. Phys.* **80**, 1972 (1984), <https://doi.org/10.1063/1.446959>.
- [22] M. R. Pederson, R. A. Heaton, and C. C. Lin, *J. Chem. Phys.* **82**, 2688 (1985), <https://doi.org/10.1063/1.448266>.
- [23] J. P. Perdew, in *Density Functional Theory of Many-Fermion Systems*, Advances in Quantum Chemistry, Vol. 21, edited by P.-O. Löwdin (Academic Press, 1990) pp. 113 – 134.
- [24] M. R. Pederson, A. Ruzsinszky, and J. P. Perdew, *J. Chem. Phys.* **140**, 121103 (2014), <https://doi.org/10.1063/1.4869581>.
- [25] M. R. Pederson, *J. Chem. Phys.* **142**, 064112 (2015), <https://doi.org/10.1063/1.4907592>.
- [26] M. R. Pederson and T. Baruah (Academic Press, 2015) pp. 153 – 180.
- [27] D.-y. Kao, K. Withanage, T. Hahn, J. Batool, J. Kortus, and K. Jackson, *J. Chem. Phys.* **147**, 164107 (2017), <https://doi.org/10.1063/1.4996498>.
- [28] D.-y. Kao, M. R. Pederson, T. Hahn, T. Baruah, S. Liebing, and J. Kortus, *Magnetochemistry* **3** (2017), 10.3390/magnetochemistry3040031.
- [29] D.-y. Kao and M. R. Pederson, *Mol. Phys.* **115**, 552 (2017), <https://doi.org/10.1080/00268976.2016.1225992>.
- [30] M. R. Pederson, T. Baruah, D.-y. Kao, and L. Basurto, *J. Chem. Phys.* **144**, 164117 (2016), <https://doi.org/10.1063/1.4947042>.
- [31] K. Sharkas, L. Li, K. Treppe, K. P. K. Withanage, R. P. Joshi, R. R. Zope, T. Baruah, J. K. Johnson, K. A. Jackson, and J. E. Peralta, *J. Phys. Chem. A* **122**, 9307 (2018), pMID: 30412407, <https://doi.org/10.1021/acs.jpca.8b09940>.
- [32] R. P. Joshi, K. Treppe, K. P. K. Withanage, K. Sharkas, Y. Yamamoto, L. Basurto, R. R. Zope, T. Baruah, K. A. Jackson, and J. E. Peralta, *J. Chem. Phys.* **149**, 164101 (2018), <https://doi.org/10.1063/1.5050809>.
- [33] K. P. K. Withanage, S. Akter, C. Shahi, R. P. Joshi, C. Diaz, Y. Yamamoto, R. Zope, T. Baruah, J. P. Perdew, J. E. Peralta, and K. A. Jackson, *Phys. Rev. A* **100**, 012505 (2019).
- [34] J. Batool, T. Hahn, and M. R. Pederson, *Journal of Computational Chemistry* (2019), 10.1002/jcc.26008.

- [35] Z.-h. Yang, M. R. Pederson, and J. P. Perdew, *Phys. Rev. A* **95**, 052505 (2017).
- [36] S. Klüpfel, P. Klüpfel, and H. Jónsson, *Phys. Rev. A* **84**, 050501 (2011).
- [37] C. Shahi, P. Bhattarai, K. Wagle, B. Santra, S. Schwalbe, T. Hahn, J. Kortus, K. A. Jackson, J. E. Peralta, K. Treppe, S. Lehtola, N. K. Nepal, H. Myneni, B. Neupane, S. Adhikari, A. Ruzsinszky, Y. Yamamoto, T. Baruah, R. R. Zope, and J. P. Perdew, *J. Chem. Phys.* **150**, 174102 (2019), <https://doi.org/10.1063/1.5087065>.
- [38] J. P. Perdew, K. Burke, and M. Ernzerhof, *Phys. Rev. Lett.* **77**, 3865 (1996).
- [39] J. P. Perdew, K. Burke, and M. Ernzerhof, *Phys. Rev. Lett.* **78**, 1396 (1997).
- [40] J. P. Perdew, K. Burke, and Y. Wang, *Phys. Rev. B* **54**, 16533 (1996); *Phys. Rev. B* **57**, 14999 (1998).
- [41] J. Sun, A. Ruzsinszky, and J. P. Perdew, *Phys. Rev. Lett.* **115**, 036402 (2015).
- [42] B. Santra and J. P. Perdew, *J. Chem. Phys.* **150**, 174106 (2019), <https://doi.org/10.1063/1.5090534>.
- [43] P. Verma, A. Perera, and R. J. Bartlett, *Chem. Phys. Lett.* **524**, 10 (2012).
- [44] M.-C. Kim, E. Sim, and K. Burke, *Phys. Rev. Lett.* **111**, 073003 (2013).
- [45] R. R. Zope, T. Baruah, and K. A. Jackson, “FLOSIC 0.1.2,” Based on the NRLMOL code of M. R. Pederson.
- [46] M. R. Pederson and K. A. Jackson, *Phys. Rev. B* **41**, 7453 (1990).
- [47] K. Jackson and M. R. Pederson, *Phys. Rev. B* **42**, 3276 (1990).
- [48] M. Pederson, D. Porezag, J. Kortus, and D. Patton, *Phys. Status Solidi (b)* **217**, 197 (2000), <https://onlinelibrary.wiley.com/doi/pdf/10.1002/%28SICI%291521-3951%28200001%29217%3A1%3C197%3>
- [49] S. Lehtola, C. Steigemann, M. J. Oliveira, and M. A. Marques, *SoftwareX* **7**, 1 (2018).
- [50] M. A. Marques, M. J. Oliveira, and T. Burnus, *Comput. Phys. Commun.* **183**, 2272 (2012).
- [51] D. Porezag and M. R. Pederson, *Phys. Rev. A* **60**, 2840 (1999).
- [52] S. Schwalbe, T. Hahn, S. Liebing, K. Treppe, and J. Kortus, *J. Comput. Chem.* **39**, 2463 (2018), <https://onlinelibrary.wiley.com/doi/pdf/10.1002/jcc.25586>.
- [53] J. P. Perdew and Y. Wang, *Phys. Rev. B* **45**, 13244 (1992).
- [54] A. P. Bartók and J. R. Yates, *The Journal of Chemical Physics* **150**, 161101 (2019), <https://doi.org/10.1063/1.5094646>.
- [55] F. Zahariev, S. S. Leang, and M. S. Gordon, *J. Chem. Phys.* **138**, 244108 (2013), <https://doi.org/10.1063/1.4811270>.

- [56] Z.-h. Yang, H. Peng, J. Sun, and J. P. Perdew, *Phys. Rev. B* **93**, 205205 (2016).
- [57] S. J. Chakravorty, S. R. Gwaltney, E. R. Davidson, F. A. Parpia, and C. F. Fischer, *Phys. Rev. A* **47**, 3649 (1993).
- [58] A. Wasserman, J. Nafziger, K. Jiang, M.-C. Kim, E. Sim, and K. Burke, *Annual Review of Physical Chemistry* **68**, 555 (2017).
- [59] A. Kramida, Yu. Ralchenko, J. Reader, and NIST ASD Team, NIST Atomic Spectra Database (ver. 5.6.1), [Online]. Available: <https://physics.nist.gov/asd> [2018, July 25]. National Institute of Standards and Technology, Gaithersburg, MD. (2018).
- [60] National Institute of Standards and Technology, NIST Computational Chemistry Comparison and Benchmark Database NIST Standard Reference Database Number 101 Release 19, April 2018, Editor: Russell D. Johnson III <http://cccbdb.nist.gov/> DOI:10.18434/T47C7Z.
- [61] L. A. Curtiss, K. Raghavachari, G. W. Trucks, and J. A. Pople, *J. Chem. Phys.* **94**, 7221 (1991), <https://doi.org/10.1063/1.460205>.
- [62] B. J. Lynch and D. G. Truhlar, *J. Phys. Chem. A* **107**, 8996 (2003), <https://doi.org/10.1021/jp035287b>.
- [63] L. Goerigk and S. Grimme, *Journal of Chemical Theory and Computation* **6**, 107 (2010), pMID: 26614324, <https://doi.org/10.1021/ct900489g>.
- [64] L. Goerigk, A. Hansen, C. Bauer, S. Ehrlich, A. Najibi, and S. Grimme, *Phys. Chem. Chem. Phys.* **19**, 32184 (2017).
- [65] M. Levy, J. P. Perdew, and V. Sahni, *Phys. Rev. A* **30**, 2745 (1984).
- [66] M. K. Harbola, *Phys. Rev. B* **60**, 4545 (1999).
- [67] T. Stein, H. Eisenberg, L. Kronik, and R. Baer, *Phys. Rev. Lett.* **105**, 266802 (2010).
- [68] D. Jacquemin, B. Moore, A. Planchat, C. Adamo, and J. Autschbach, *J. Chem. Theory Comput.* **10**, 1677 (2014), pMID: 26580376, <https://doi.org/10.1021/ct5000617>.
- [69] M. Levy and J. P. Perdew, *Phys. Rev. A* **32**, 2010 (1985).
- [70] P. Linstrom and W. Mallard, Eds., NIST Chemistry WebBook, NIST Standard Reference Database Number 69, National Institute of Standards and Technology, Gaithersburg MD, 20899, <https://doi.org/10.18434/T4D303>, (retrieved March 19, 2019).
- [71] K. P. Huber and G. Herzberg, *Molecular Spectra and Molecular Structure*, Vol. 4. Constants of diatomic molecules (Van Nostrand Reinhold, New York, 1979).